

# Neutron small angle scattering on Udimet 720 Ni superalloy turbine blade. Non destructive analysis of the $\gamma'$ precipitation

P. BIANCHI, D.D'ANGELO, C.R.T.N. ENEL, Milano, Italy. F. CARSUGHI, F. RUSTICHELLI, Istituto di Fisica Medica, Università di Ancona, Italy. M. MAGNANI, M. STEFANON, E.N.E.A. Bologna, Italy.

## Abstract

An investigation on thermal treatment effects on Udimet 720 Ni superalloy was performed by using neutron small angle scattering. In particular  $\gamma'$  precipitation was considered. The sample was obtained from a turbine blade used in a generator of electricity power. The measurement was performed at the D11 in the Institute Laue Langevin in Grenoble. The neutron wavelength was  $\lambda = 1$  nm. The microstructural data were compared with those obtained by transmission electron microscopy. A satisfactory agreement appeared in the size distributions obtained by using the two techniques. The feasibility of non destructive microstructural tests was so demonstrated.

## Riassunto

**Analisi non distruttiva mediante diffusione neutronica a piccoli angoli della precipitazione  $\gamma'$  in una paletta di turbina di una superlega di Ni Udimet 720.**

È stato condotto uno studio sull'effetto del trattamento termico su una superlega di Nichel, con la tecnica della diffusione neutronica a piccoli angoli. In particolare è stata considerata la fase precipitata  $\gamma'$ . Il campione è stato ottenuto da una paletta di turbina usata in generatori di energia elettrica.

L'esperimento è stato effettuato presso l'Istituto Laue Langevin di Grenoble (Francia) utilizzando il diffrattometro D11.

La lunghezza d'onda dei neutroni era di 1 nm.

I risultati della microstruttura sono confrontati con quelli ottenuti per mezzo della microscopia elettronica in trasmissione.

Tale confronto tra le due tecniche ha fornito un soddisfacente accordo per quanto riguarda le distribuzioni dimensionali dei precipitati.

È stata così dimostrata la possibilità di effettuare un'analisi microstrutturale non distruttiva utilizzando la diffusione neutronica.

## Introduction

The precipitated  $\gamma'$  phase in Nickel Superalloy is associated with strengthening of the material widely used in several technological applications as in the turbine blades of the turbogas power plants working at high temperature (over 850°C). The presence of gas and combustion products together with thermal gradients, due to the transients, produce very high stress fields and corrosive attack. Of particular interest to this study is the work of Cortese et al. (1978) (1) who did investigate at FIAT a set of samples of some Nickel Superalloys by using Small Angle Neutron Scattering (SANS) and Transmission Electron Microscopy (TEM).

Aim of present paper is to report the results of an investigation of the precipitated phases in a Nickel Superalloy Udimet 720, quite different from those previously mentioned. Also in this case the Small Angle

Neutron Scattering technique, supported by the complementary transmission electron microscopy, was used in non-destructive way to evaluate volumetric fraction of  $\gamma'$  phase and the size distribution of  $\gamma'$  precipitates. This work constitutes a much more complete investigation as compared to the preliminary results obtained on the same samples by using Double Crystal Diffractometer (DCD) (2).

## Materials

Udimet 720 is a Nickel based forged superalloy constituted of a bimodal matrix of  $\gamma$  phase with a precipitation of  $\gamma'$  phase. The  $\gamma$  phase is a solid solution of nickel, chromium, cobalt and other elements (3). The  $\gamma$  and  $\gamma'$  phases have a face centered cube (fcc) lattice with a lattice parameter respectively of 0.352 nm and 0.358 nm. In Tab. 1 are reported the chemical

**Table 1. Chemical compositions and proposed  $\gamma'$  stoichiometry**  
**Chemical composition (wt %)**

Element	Ni	Co	Mo	W	Cr	Al	Ti	C	Fe	Si
Material	56.10	14.00	3.30	1.30	17.80	2.50	4.80	0.04	0.16	0.2
$\gamma$	47.03	19.41	4.89	—	27.51	0.68	0.48			
$\gamma'$	70.16	5.34	1.97	4.99	2.52	5.19	9.83			

## Proposed stoichiometry

$(\text{Ni}_{0.894}\text{Co}_{0.068}\text{Mo}_{0.015}\text{W}_{0.020}\text{Cr}_{0.003})_3(\text{Al}_{0.431}\text{Ti}_{0.469}\text{Cr}_{0.100})$



compositions of the material, of the  $\gamma$  and  $\gamma'$  phases, as well as a proposed  $\gamma'$  stoichiometry. Other second phases are essentially constituted of large carbides ( $10\mu\text{m}$ ) containing Ti and Mo. SANS experiments have been performed on a heat treated sample taken from a turbine blade, and on a virgin one without any thermal treatment (4).

Fig. 1 - TEM observation of primary and secondary  $\gamma'$  phase.

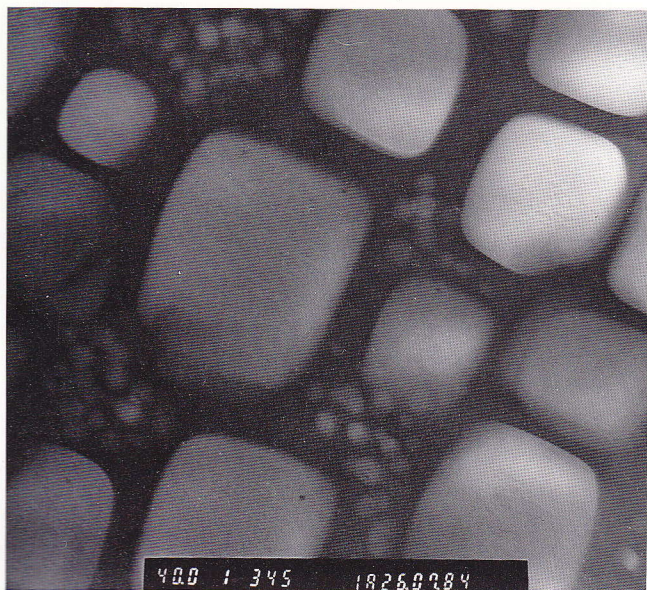
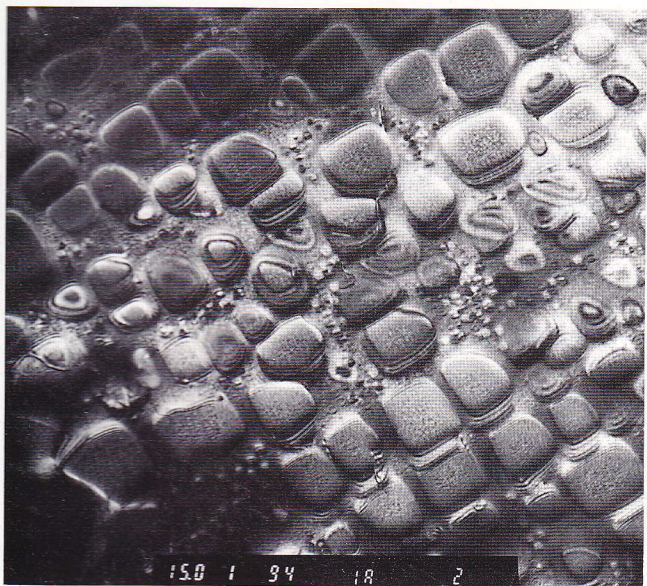


Fig. 2 - TEM observation of Turbine Blade sample.



## Transmission electron microscopy observations

Microstructural investigation by TEM allows at first to evict  $\gamma$  matrix and primary and secondary  $\gamma'$  phase. Inside the same chemical composition the  $\gamma'$  phase shows different dimensions and morphologies (Fig. 1): the primary  $\gamma'$  has a cuboidal form with average dimension of about 500 nm; secondary  $\gamma'$  is spheroidal with mean diameter of about 50 nm. The heat treated material (Fig. 2), presents within the  $\gamma$  matrix a packed and regular precipitation of primary  $\gamma'$ , surrounded by secondary  $\gamma'$ . The virgin material (Fig. 3), has a microstructure constituted by wide dimensional range of  $\gamma$  grains; moreover  $\gamma'$  phase too is not so regularly distributed.

## Small angle neutron scattering

### Experimental technique

The measurements of SANS were performed on the D11 instrument at High Flux Reactor of Institute Laue Langevin (ILL) in Grenoble (Fig. 4). The wavelength used was  $\lambda = 1 \text{ nm}$  which avoids double Bragg scattering. Two distances sample-to-detector (40 m and 10 m), and two distances of collimation (40.5 m and 10.5 m) were employed. These values yield to a range of exchanged wave vector

$$7 \times 10^{-3} \leq Q \leq 2.3 \times 10^{-1} \text{ nm}^{-1},$$

Fig. 3 - TEM observation of Virgin sample.

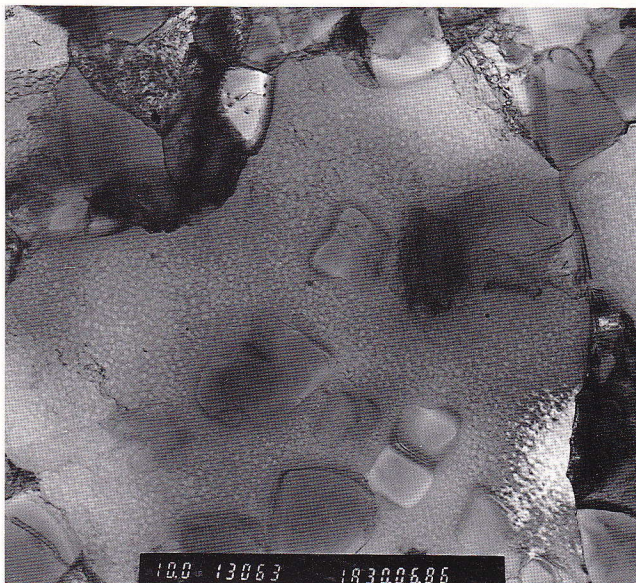
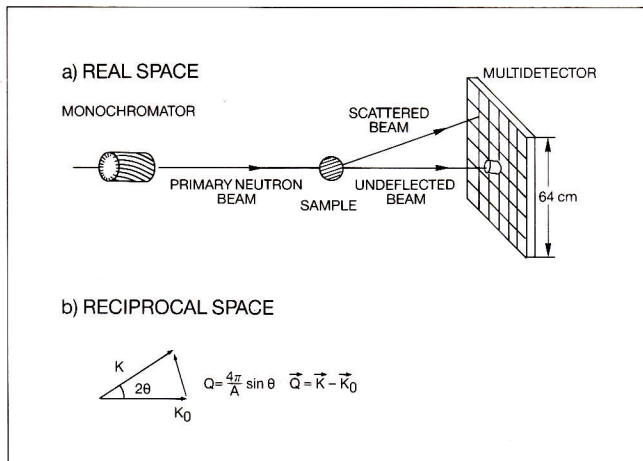




Fig. 4a - Schematic arrangement of Small Angle Scattering camera D11 at High Flux Reactor in Grenoble.

Fig. 4b - The exchanged wave vector  $Q$ :  
 $K_0$  is the wave vector of the incident beam.  
 $K$  is the wave vector of the scattered beam.



where the exchanged wave vector is defined by

$$Q = \frac{4\pi}{\lambda} \sin \theta,$$

the take-off angle being expressed by  $2\theta$ . To obtain the absolute cross section a calibration was performed with water in a quartz cell involving the incoherent scattering cross section of water, which is well known. The data were treated with standard procedures available in Grenoble. The theory of SANS for non destructive test can be found in Kostorz (1979) (5) and Walther & Pizzi (1980) (6).

The coherent absolute cross section  $d\Sigma/d\Omega(Q)$  was calculated by the equation

$$\frac{d\Sigma}{d\Omega}(Q) = \frac{d_w \cdot T_w}{d_s \cdot T_s} \cdot \frac{(I_s - b) - (T_s/T_h) \cdot (I_h - b)}{(I_w - b) - (T_w/T_q) \cdot (I_q - b)} \cdot (d\Sigma/d\Omega)_w$$

where  $d$  and  $T$  represent the thickness and the transmission and  $w, s, b, h, q$  are indexes which refer to water, sample, background, hole (without sample) and empty quartz cell, respectively. The value of the incoherent macroscopic cross section of water  $(d\Sigma/d\Omega)_w$  was determined by Oberthür (7) at ILL in Grenoble.

### Theoretical background

At low  $Q$  values the dependence of the scattering profile due to precipitate particles is given under some

restrictive assumptions (8) by the Guinier law

$$\frac{d\Sigma}{d\Omega}(Q) \div \exp \{ -Q^2 \cdot R_g^2/3 \} \quad (1)$$

i.e. the plot of  $\ln(d\Sigma(Q)/d\Omega)$  versus  $Q^2$  is characterized by the slope

$$m = -R_g^2/3$$

where  $R_g$  is the Guinier Radius of the particles. As the validity of Eq. 1 is restricted to cases without interference effects between particles, it has no clear meaning to apply it to a dense system of precipitates, as in the case of the turbine blade sample. At large  $Q$  values the Porod law is valid, which foresees an asymptotic  $Q^{-4}$  dependence, for  $d\Sigma(Q)/d\Omega$ , which allows the determination of the total surface per unit volume  $S$ :

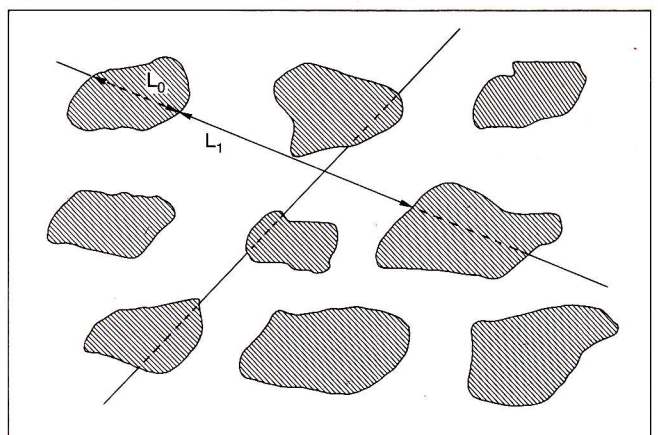
$$\frac{d\Sigma}{d\Omega}(Q) = (\Delta\rho)^2 \cdot 2\pi \cdot S \cdot Q^{-4} \quad (2)$$

where  $(\Delta\rho)$  is the difference of scattering length density between precipitates and matrix. The precipitated volume fraction  $C$  is also easily obtained by the equation:

$$2\pi^2 \cdot (\Delta\rho)^2 \cdot C = \int_0^\infty Q^2 \cdot \frac{d\Sigma}{d\Omega}(Q) \cdot dQ \quad (3)$$

As the absolute scattering cross section  $d\Sigma(Q)/d\Omega$  is in practice measured only for a finite  $Q$  range, in order to evaluate the integral appearing in Eq.3, an extrapolation to zero value and to infinite value of  $Q$  is necessary by using the Guinier law and the Porod law, respectively. The presence of interference introduces some modifications (especially in the  $Q$  range around the

Fig. 5 - Average linear dimensions  $L_0$  and  $L_1$  in a two phase system.



value  $Q \cdot R_0 \approx 2$ , where  $R_0$  is the particle radius) in the behaviour of the scattering curve in comparison to the one of a dilute system, so that in this case some approximations are involved in the results obtained by using Eq. 1, 2 and 3. For a very packed system, like the turbine blade sample, it is convenient to introduce a physical quantity called Correlation Length  $L$  defined by

$$\frac{1}{L} = \frac{1}{L_0} + \frac{1}{L_1} \quad (4)$$

where,  $L_0$  and  $L_1$  are the average values of the chords defined in Fig. 5. It can be shown that the correlation length  $L$  is connected to the neutron cross section by

$$2\pi \cdot (\Delta\rho)^2 \cdot C \cdot (1 - C) \cdot L = \int_0^\infty Q \cdot \frac{d\Sigma}{d\Omega}(Q) \cdot dQ \quad (5)$$

## Results and discussion

### Guinier Radii

The analysis of the experimental scattering profiles (Fig. 6) by means of Eq. 1 shows a Guinier Radius  $R_{gv} \approx 230$  nm in the case of virgin sample and  $R_{gt} \approx 150$  nm in the case of the turbine blade. This is in disagreement with what expected and with the results of TEM observations which show the presence of more large particles in the turbine blade. This fact can be easily justified as a consequence of strong interference, which will be certainly present for a densely packed precipitate structure like the one in the

Fig. 6 - Scattering curves for Turbine Blade sample (o) and Virgin sample (●).

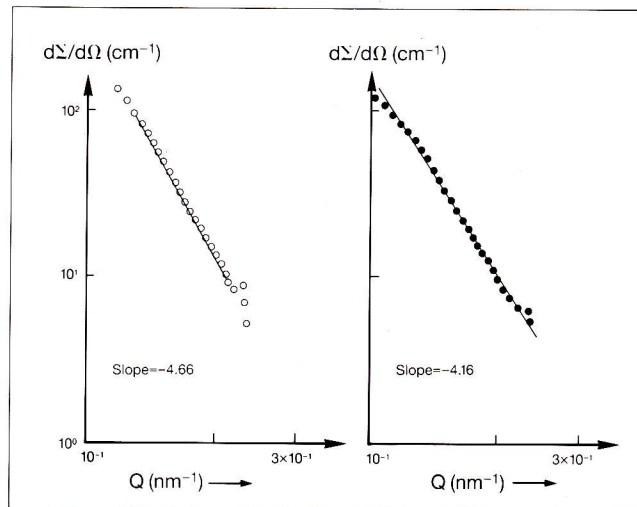
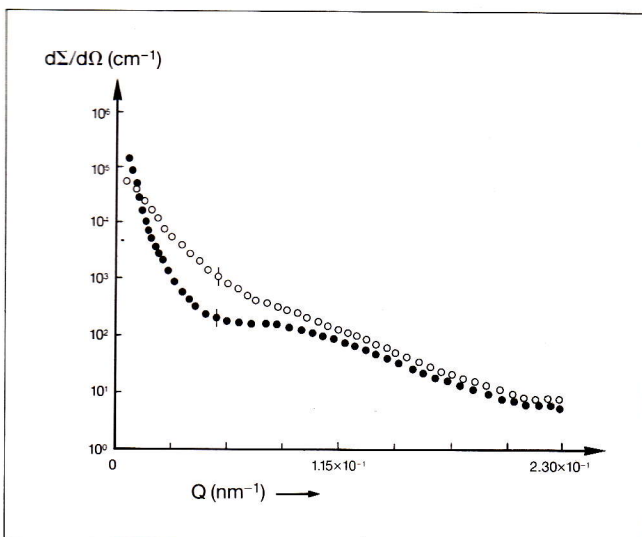


Fig. 7 - Check of the Porod law for Turbine Blade sample (o) and Virgin sample (●).

turbine blade and which reduces the  $R_{gt}$  value. In conclusion the obtained Guinier Radius of the virgin sample appears to be reasonable whereas the one of the turbine blade sample is approximated but of the same order of magnitude of the real value.

### Total surface

The applicability of the Porod law was tested looking at the asymptotic slope of log-log plot of the scattering profile (Fig. 7). In fact from Eq. 2 one obtains

$$\log(d\Sigma/d\Omega) = -4 \cdot \log Q + k$$

where  $k = \log(2\pi \cdot S \cdot (\Delta\rho))$ , so that the asymptotic slope  $m_p$  must be equal to  $-4$ . The obtained values are

$$m_{pt} = -4.66 \text{ for the turbine blade}$$

$$m_{pv} = -4.16 \text{ for the virgin sample.}$$

From equation 2 it is possible to obtain the total surface  $S$  of the precipitate per unit volume by

$$S = \frac{1}{2\pi \cdot (\Delta\rho)^2} \cdot (d\Sigma/d\Omega)_{\text{asympt.}} \quad (6)$$

It should be noted that equation 6 is influenced only by the asymptotic behaviour of the scattering profile which is not connected to some interference effects.

The values of  $S_v = 28.5 \text{ m}^2/\text{cm}^3$  for the virgin sample and  $S_t = 38.3 \text{ m}^2/\text{cm}^3$  for the turbine blade sample were found.



A rough independent evaluation of these quantities was performed by using a simple geometrical model for the sample, which is assumed to consist only of secondary  $\gamma'$  precipitates imbedded in the matrix. The  $\gamma'$  primary precipitates were neglected because the ratio between the number of primary and secondary precipitates is about  $10^{-3}$  for both samples. Moreover in the model a value of 19 nm was assumed for the precipitate radius of the virgin sample and of 23 nm in the case of the turbine blade sample and a volume fraction of 0.18 and 0.35, respectively. These four values were obtained from the data evaluation reported in the next two sections. A value of  $S_v = 28.4 \text{ m}^2/\text{cm}^3$  was obtained for the virgin sample and of  $S_t = 45.6 \text{ m}^2/\text{cm}^3$  for the turbine blade sample, by simple geometrical evaluations: a satisfactory agreement is there found with the values obtained from the neutron data. The values of the asymptotic slope are sufficiently close to  $-4$  to justify, as a first approximation, the calculation of the integral in Eq. 3 by extrapolating the scattering profile with the Porod law.

### Volume fraction

The volume fraction for the two investigated samples was obtained from the experimentally obtained cross section  $d\Sigma(Q)/d\Omega$  through Eq. 3. The extrapolation to zero  $Q$  value of the scattering curve was performed, as already mentioned by the Guinier law (Eq. 1) and to large  $Q$  values by the Porod law (Eq. 2). A certain approximation is introduced in the low  $Q$  value extrapolation by the interference effects: however the weighing  $Q^2$  factor appearing in the integral in Eq. 3 reduces strongly the approximations in  $d\Sigma(Q)/d\Omega$ . The values of the integral are  $2.8616 \cdot 10^{-8} \text{ nm}^{-4}$  and  $5.5729 \cdot 10^{-8} \text{ nm}^{-4}$  for the virgin sample and for the turbine blade sample, respectively, leading to a precipitate volume fraction  $C_v = 0.18$  for the virgin sample and  $C_t = 0.35$  for the turbine blade sample. It could be shown that the involved approximations in the neutron data analysis lead to underestimation.

### Particle size distribution

A different approach to the analysis of scattering profiles consists in fitting to the experimental data calculated profiles obtained assuming a polydisperse set of particles of given shape (Fig. 8). If interference is negligible the coherent neutron cross section due to precipitates is given by

$$\frac{d\Sigma}{d\Omega}(Q) = (\Delta\rho)^2 \cdot \int_0^\infty N(R) \cdot V^2(R) \cdot G^2(QR) \cdot dR \quad (7)$$

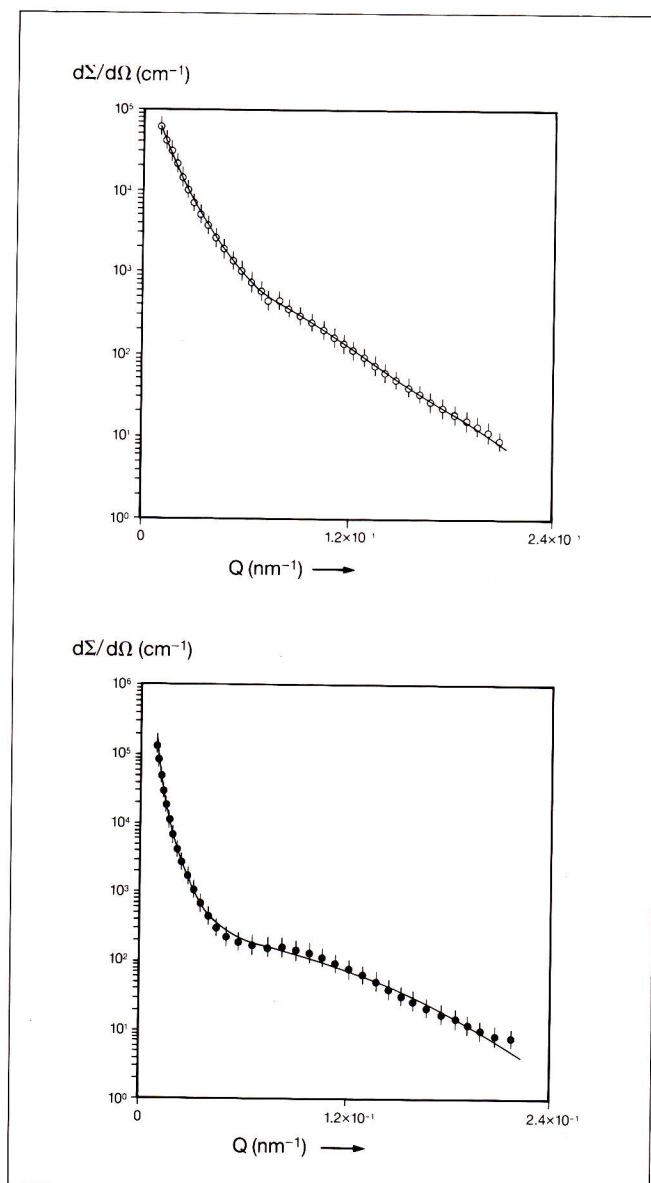


Fig. 8 - Best fit associated with Turbine Blade sample (o) and Virgin sample (●).

where  $G(QR)$  is the direction averaged scattering function of a precipitate of the assumed shape and of size  $R$ ,  $V(R)$  is the precipitate volume,  $N(R)$  is the size distribution (i.e.  $N(R)dR$  is the number of particles having size between  $R$  and  $R+dR$ ) and  $\Delta\rho$  is the scattering length contrast. This approach is not so strongly affected by the limitation of the measurement range as the preceding analysis but is limited by the validity of the main assumptions i.e.

- 1) precipitates have a unique known shape
- 2) the effects of different precipitates add incoherently.

As precipitates are supposed to be not strongly elongated the form factor  $G(QR)$  is approximated by that of a sphere of radius  $R$

$$G^2(QR) = \frac{9}{2} \cdot \pi \cdot \frac{J_{3/2}^2(QR)}{(QR)^3} \quad (8)$$

The size density function  $N(R)$  was approximated by a linear combination of  $\beta$ -cubic splines with knots equispaced in  $z = \log R$  i.e.

$$N(R) = \sum_1^{N_k} C_k \cdot \phi_k(z) \quad (9)$$

and a constrained least square fitting code was used to optimize the  $c_k$  values. If no constraints are present, the least square problem is a linear one, in fact from Eq. 7 and 9 one has:

$$\frac{d\Sigma}{d\Omega}(Q) = (\Delta\rho)^2 \cdot \sum_1^{N_k} C_k \cdot \phi_k(Q)$$

where

$$\phi_k(Q) = \int_0^\infty V^2(R) \cdot G^2(QR) \cdot \phi_k(\log R) \cdot dR \quad (10)$$

However, two major complications are to be faced. The first one is that, usually, the least square problem becomes nearly ill conditioned if a large number of splines, i.e. of parameters  $c_k$ , is used. The second one is the positive nature of the size distribution  $N(R)$  which would have otherwise no physical meaning. Both difficulties are faced by means of a regularization technique which makes use of a variable damping constraint. This method was employed in earlier works (10) (11) and is more extensively described in (12). The method allows also an estimate of errors in the adjusted size distribution. This makes use of the inverse of the normal equation matrix (covariance matrix) disregarding the effect of damping and of the constraint to positive  $N(R)$  values and is then an overestimate of real errors. The analysis of the virgin sample shows two families of precipitates (Fig. 9) centered around  $R = 19$  nm and  $R = 260$  nm, in perfect agreement with those observed in TEM measurements. The corresponding precipitated volume fraction is  $V_c = 0.15$ . The turbine blade sample leads to a more complicated result (Fig. 10). A  $\gamma'$  phase centered around 20 nm is always present but an almost continuous distribution appears in the range  $40 \text{ nm} < R < 400 \text{ nm}$  with a reduction of the contribution to the precipitated volume fraction of very large precipitates ( $R \approx 200\text{-}300$  nm). This seems in clear contradiction with TEM results which show a close packed structure of large precipitates ( $R \approx 250$

Fig. 9 - Logarithmic volume distribution for the Virgin sample.

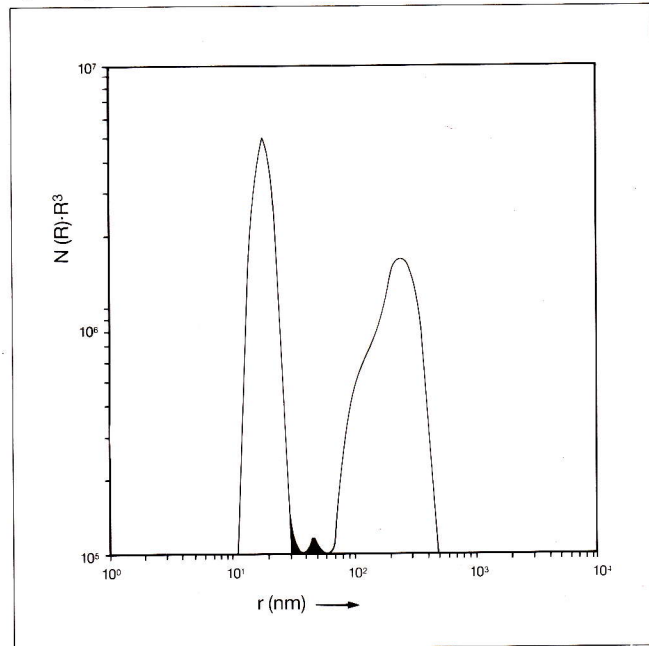
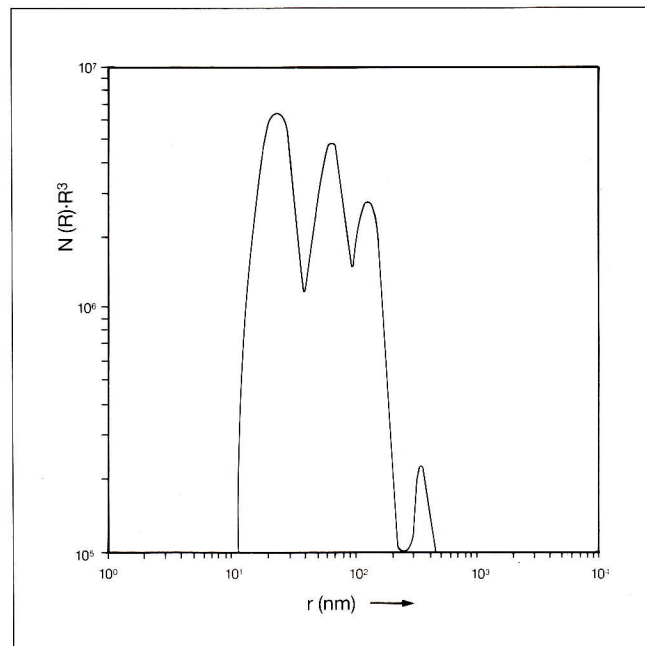


Fig. 10 - Logarithmic volume distribution for the Turbine Blade sample.



nm). A possible interpretation should be looked for in the effect of interference which in such cases, in agreement with the Babinet principle, leads to an effective size (average chord) depending on both phase and interphase dimensions (6). A more thorough study



of close packed structure, taking account of interference, is in progress. The precipitated volume fraction corresponding to the size distribution of Fig. 10 is 0.35, in perfect agreement with the results of preceding evaluations.

## Conclusions

Microstructural data were obtained by neutron small angle scattering concerning the  $\gamma'$  precipitation in a turbine blade and in a virgin sample of Udimet 720. In particular the Guinier radii, the total surface per unit volume, the volume fraction, the correlation length and the size distribution of  $\gamma'$  precipitates were obtained.

The data appear to be coherent and in satisfactory agreement with TEM results. In spite of the approximations involved, consisting mainly in disregarding interference, the order of magnitude of the results are fully acceptable and, for the virgin sample, for which the assumptions are more justified, a satisfactory quantitative agreement is found.

Compared with other works on superalloys (1) it should be noted the high resolution achieved with the D11 equipment at the High Flux Reactor in Grenoble, which allows to detect precipitates whose dimensions are of the order of magnitude of  $10^2$  nm. In conclusion, this experiment shows that the SANS is a powerful non-destructive technique, providing information on the evolution of the microstructure of Ni-superalloys resulting from thermal treatments. In perspective this SANS technique could be routinely used in order to reveal the accumulation of damage in the behaviour of technological materials during their exploitation.

## Acknowledgments

The authors are grateful to Prof. G. Caglioti and Prof. S. Melone for useful discussion; to Mr. M. Pergolini and Mr. S. Polenta for valuable technical assistance.

## REFERENCES

- (1) Cortese, P., P. Pizzi, H. Walther, G. Bernardini, and A. Olivi. Non-Destructive Characterization of Turbine Blades and Nickel Alloys by Small Angle Neutron Scattering. *Material Sciences and Engineering*, **36** (1978), 81.
- (2) Bianchi, P., F. Carsughi, D. D'Angelo, J. Kulda, A. Mengoni, P. Mikula, and F. Rustichelli. Non-destructive analysis of the  $\gamma'$  precipitation in a Udimet 720 turbine blade by SANS. *Material Science Forum*, in print.
- (3) Ramous, E. *Contratto di ricerca ENEL-CRTN, Università di Padova* (1984-85).
- (4) D'Angelo, D. *Progetto finalizzato CNR - Metallurgia. Esecutivo 1983. Rapporto tecnico semestrale di avanzamento 1 Giugno 1984 - 31 Dicembre 1984* (1985).
- (5) Kostorz, G. Small Angle Scattering and its applications to material sciences. In G. Kostorz (Ed.), *Neutron Scattering*, Academic Press, New York, 1979, vo. 15. p. 227.
- (6) Walther, H., and A. Pizzi. Small Angle Neutron Scattering. In R.S. Sharpe (Ed.), *Research Techniques in Nondestructive Testing*, Academic Press, New York, 1980, p. 341.
- (7) Oberthür, R. *Private communication*, ILL, Grenoble (1982).
- (8) Guinier, A., and J. Fournet. General Theory. *Small Angle Scattering of X-rays*, John Wiley, New York, 1955, 5.
- (9) Porod, G. *Kolloid Z.*, **124** (1951), 83, 114.
- (10) Abis, S., A. Boeuf, R. Caciuffo, P. Fiorini, M. Magnani, S. Melone, F. Rustichelli and M. Stefanon. Investigation of  $Mg_2Si$  precipitation in an Al-Mg-Si alloy by Small Angle Neutron Scattering. *Journal of Nuclear Material*, **135** (1985), 181.
- (11) Abis, S., R. Caciuffo, R. Coppola, M. Magnani, F. Rustichelli, and M. Stefanon. Small angle neutron scattering investigation of the ageing process in Al-Mg-Si alloy. *Physica*, **136B** (1986), 469.
- (12) Stefanon, M. To be published.